

# Numerical Analysis of the Decomposition Method Using LTE Reference Antennas

Bernhard Auinger, Michael Gadringer, Adam Tankielun, Christoph Gagern, and Wolfgang Bösch

**Abstract**—In this document a numerical validation of the decomposition method is presented. This is a powerful method to split MIMO (multiple input multiple output) enabled UE (user equipment) tests in a radiated and a conducted part to save measurement time.

The concept and fundamental properties of this procedure are introduced. The aim is to show the validity under certain circumstances of this concept by simulation.

The chosen path is to employ a  $2 \times 2$  MIMO transmission system. Stochastic and deterministic channel models are used, as Rayleigh channels with no line of sight components (NLOS) and identity matrices. Receiving antenna setups with different characteristics were investigated.

Also the practical behaviour of the method using CTIA (The Wireless Association) LTE (Long Term Evolution) reference antennas has been examined. Therefore the distributions of the antenna condition number and of the deviation between the results are provided.

**Index Terms**—Decomposition method, decomposition approach, LTE, LTE device test, MIMO, MIMO OTA test, OTA, two-channel method.

## I. INTRODUCTION

Both LTE device suppliers and network operators need quantitative test methods for rating the performance of the wireless user equipment. These verifications should include all parts, like antennas, filters, amplifiers and implementation of the receiver algorithms. The user equipment validation should be done radiated in three dimensions and channel fading has to be included. Hence, lots of data has to be transferred to get repeatable results at every position of the test antennas. Results are accurate, but very time consuming.

The decomposition method takes another approach and dramatically reduces the test time for a test of a single unit.

## II. DECOMPOSITION METHOD

The method is introduced in [1], [2]. It employs the two-channel method (Fig. 1) for radiated tests [3], [4]. Two test antennas are placeable in the zenith angle ( $\Theta$ -plane), the UE (user equipment) is turnable in the azimuth angle ( $\Phi$ -plane). The whole setup is placed in an anechoic chamber.

The positions of the UE, as well as the test antenna placement and their polarizations are defined in so called constellations. The quiet zone is defined as the area where the

user equipment has to be placed [5].

The result of these measurements is downlink power  $P$  as a function of relative data throughput  $y$ :  $P(y)$ . Instead of doing one single radiated faded test at every constellation, measurements are split in three parts:

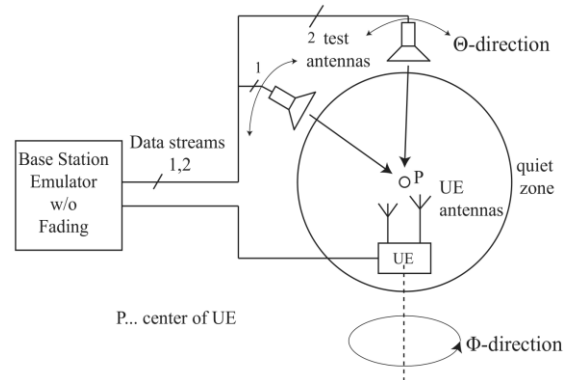


Fig. 1. Scheme of the decomposition method measurement setup.

- A conducted test, no fading is applied: 'Baseline'-result  $P_{bl}(y)$  (Fig. 2(d))
- A conducted test, using fading: 'Channel'-result  $P_{ch}(y)$  (Fig. 2(c))
- A radiated test, no fading is applied: 'Antenna'-result  $P_{ant}(y)$  (Fig. 2(b))

The conducted tests have to be done only once, which is the clue of the method. Radiated measurements without fading have to be done at every constellations. They can be executed faster than the radiated faded ones.

All three results  $P_{bl}(y)$ ,  $P_{ch}(y)$  and  $P_{ant}(y)$  are finally combined to the decomposition method result  $P_{dc}(y)$  (dc..decomposition).

$$P_{dc}(y) = P_{ant}(y) \frac{P_{ch}(y)}{P_{bl}(y)}$$

By using logarithmic power values the deviation can be computed with summation and subtraction.

$$P_{dc,log}(y) = P_{ant,log} + P_{ch,log}(y) - P_{bl,log}(y)$$

The decomposition method result  $P_{dc}(y)$  is ideally equal to the radiated faded result  $P_{oa}(y)$  (oa..overall).

$$P_{dc}(y) = P_{oa}(y)$$

In this paper the validity of this method is shown under given circumstances. In this section the simulation framework is introduced and explained. The whole simulation environment has been implemented in MATLAB,

Manuscript received September 5, 2014; revised July 12, 2015.

Bernhard Auinger, Michael Gadringer, and Wolfgang Bösch are with the Institute of Microwave and Photonic Engineering at the Graz University of Technology, Austria (e-mail: Bernhard.auinger@tugraz.at).

Adam Tankielun and Christoph Gagern are with the Rohde & Schwarz GmbH & Co. KG, Munich, Germany.

as it provides full access to all points within the transmission system.

### III. SIMULATION SETUP

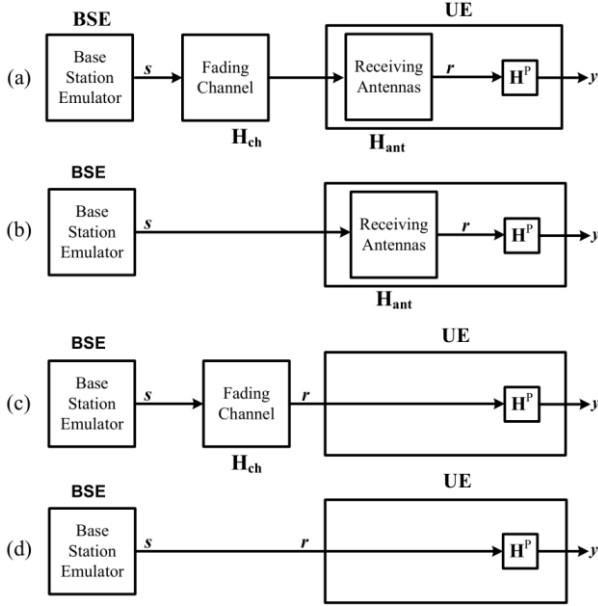


Fig. 2. Block diagram of the transmission system.

The evaluated transmission system is applying QPSK (quadrature phase shift keying) in the base station emulator (BSE). QPSK has exemplarily been selected because of its use in the LTE protocol.

The simulation uses matrix equations to describe the transmission system with transmission and reception. The data signals use a  $2 \times 2$  MIMO radio channel. As the downlink stream is simulated, the data is generated in the BSE, is transmitted over the channel, and received by the UE with its antennas (Fig. 2(d)).

A linear receiver type has been employed, namely the Zero Forcing (ZF) / Inverse Channel Detector (ICD) [6]. It is designated in the receiver with  $H^p$  (Fig. 2). The symbols are determined applying minimum Euclidian distance algorithms without prior knowledge.

#### A. Transmission Schemes

For successful application of the decomposition method in measurements, three different types of measurements have to be performed and are combined to get the final result. The same principle is applied in simulations. The used types are:

- 'Baseline'-simulation result  $P_{bl}(y)$  (Fig. 2(d))
- 'Channel'-simulation result  $P_{ch}(y)$  (Fig. 2(c))
- 'Antenna'-simulation result  $P_{ant}(y)$  (Fig. 2(b))

'Overall' simulation results  $P_{oa}(y)$  (Fig. 2(a)) are compared to the decomposition method result ( $P_{dc}(y)$ ).

#### B. Transmitted Data Configuration and Figures of Merit

The necessary figures of merit (FOM) are introduced in this section, as well as how they can be calculated:

- 1) Transmission data block size: The transmitted data streams have a length of 28 bits for one realization.
- 2) Subframe Error Rate (SFER): The transmitted (TX) bit stream is compared to the received bit stream (RX).

This is done in windows with the size of  $2^4$  bits, so-called subframes (SF). If the RX subframe completely matches the

TX subframe, it is recognized as correct. If there are one or more bits wrong, the complete subframe is rated wrong. The mathematical formulation of the subframe error rate (SFER) is

$$SFER = \frac{\text{number of correctly received SF}}{\text{number of all transmitted SF}}$$

- 3) Relative Throughput (RTP): The relative throughput is calculated by subtracting the SFER from one.

$$RTP = 1 - SFER$$

It ranges from 0 (no subframe transferred correctly) to 1 (all data transferred correctly).

#### C. Channel Matrices

In general, channels with flat frequency fading have been applied. This results in  $2 \times 2$  channel matrices, where a channel element  $h_{ij}$  simply represents the complex gain. The channel matrix elements have complex normal distributions, independent from each other. This means that the amplitude is Rayleigh distributed and the phase is independent and identically distributed (IID). It has been assumed, that no intersymbol interference (ISI) is taking place. The following channel matrices have been employed:  $H_{ch}$  is set to identity matrix for a system check

$$H_{ch} = \begin{bmatrix} 1 & 0 \\ 0 & 1 \end{bmatrix}$$

The Rayleigh fading channels with no line of sight component (NLOS) and cross coupling between the paths

$$H_{ch} = \begin{bmatrix} h_{ch,11} & h_{ch,12} \\ h_{ch,21} & h_{ch,22} \end{bmatrix}$$

For the 'Channel' and 'Overall' simulations.

The Rayleigh distribution is characterized by the parameter  $\sigma$ , it was set to 0.4. This leads to an average channel matrix of

$$H_{ch} = \begin{bmatrix} \sigma\sqrt{\frac{\pi}{2}} & \sigma\sqrt{\frac{\pi}{2}} \\ \sigma\sqrt{\frac{\pi}{2}} & \sigma\sqrt{\frac{\pi}{2}} \end{bmatrix} \cong \begin{bmatrix} 0.5 & 0.5 \\ 0.5 & 0.5 \end{bmatrix}$$

The energy of the averaged channel matrix has been calculated with the squared Frobenius Norm [6]

$$\|H_{ch}\|_{frob}^2 = \sum_{i=1}^2 \sum_{j=1}^2 |h_{ch,ij}|^2 \cong 1$$

And is approximately one, while the identity matrix energy is two. This reflects the fact, that the transmission using an identity matrix needs less downlink power than employing an NLOS channel.

#### D. Antenna Matrices

This simulation approach uses the two-channel method and only takes the influence of the receiving antennas into

account. The matrix  $\mathbf{H}_{\text{ant}}$  is calculated with the complex E-field pattern of the receiving antenna [3], [7].

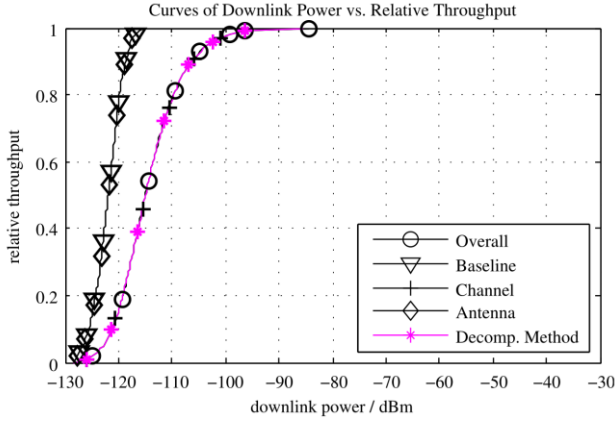


Fig. 3. Relative Throughput (RTP) vs. downlink power,  $\kappa=0\text{dB}$ .

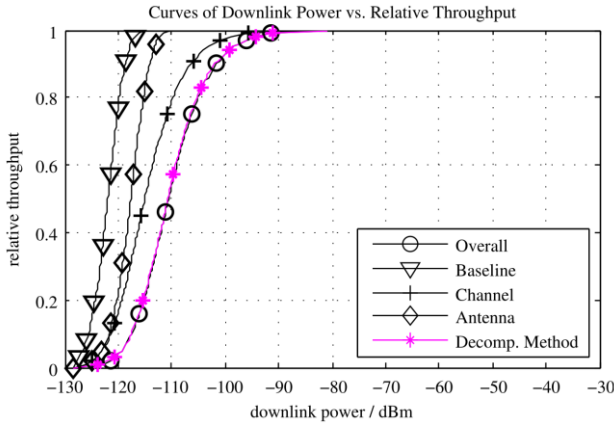


Fig. 4. Relative Throughput (RTP) vs. downlink power,  $\kappa=10\text{dB}$ .

$$\mathbf{H}_{\text{ant}} = \begin{bmatrix} h_{\text{ant},1,1} & h_{\text{ant},1,2} \\ h_{\text{ant},2,1} & h_{\text{ant},2,2} \end{bmatrix} = A \begin{bmatrix} R_{p1}(\Omega_1) & R_{q1}(\Omega_2) \\ R_{p2}(\Omega_1) & R_{q2}(\Omega_2) \end{bmatrix}$$

$R$  denotes the complex E-field pattern of the receiving antenna 1 or 2.  $p$  and  $q$  can be either  $\Theta$ - or  $\Phi$ -polarization. The factor  $A$  is used for normalization of the matrices to a squared Frobenius Norm (SQFN) of two.

$$A \|\mathbf{H}_{\text{ant}}\|_{\text{fro}}^2 = A \sum_{i=1}^2 \sum_{j=1}^2 |h_{\text{ant},ij}|^2 = 2$$

Normalization is important for the possibility to compare the behaviour of different receiving antenna matrices with different condition number  $\kappa$  under the same conditions. The condition number is an important figure of merit to describe the coupling between the antennas. It is calculated with the largest and the smallest eigenvalue of the antenna matrix  $\mathbf{H}_{\text{ant}}(\Omega_1, \Omega_2)$ . The bigger it is, the worse the matrix conditioning.

$$\kappa_{\text{lin}} = \frac{\sigma_{\text{max}}}{\sigma_{\text{min}}}$$

For better visualization  $\kappa$  is used in logarithmic terms

$$\kappa_{\text{log}} = 20 \log_{10} \left( \frac{\sigma_{\text{max}}}{\sigma_{\text{min}}} \right)$$

The identity antenna matrix corresponds to fully decoupled antennas, with  $\kappa_{\text{log}} = 0$ . Increasing coupling between the antennas provide antenna matrices with higher condition numbers, as depicted in Table I.

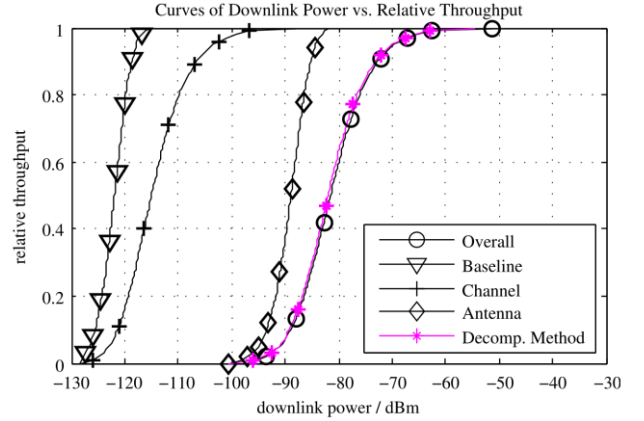


Fig. 5. Relative Throughput (RTP) vs. downlink power,  $\kappa=40\text{dB}$ .

TABLE I: KEY NUMBERS AND RESULT FIGURES OF THE SIMULATIONS

Sim. No.	$\mathbf{H}_{\text{ant}}$	$\kappa_{\text{log}} / \text{dB}$	Rec. Type	Fig.
1	$\begin{bmatrix} 1 & 0 \\ 0 & 1 \end{bmatrix}$	0	ZF/ICD	3
2	$0.8874 \begin{bmatrix} 1 & 0.51949 \\ 0.51949 & 1 \end{bmatrix}$	10	ZF/ICD	4
3	$0.71414 \begin{bmatrix} 1 & 0.9802 \\ 0.9802 & 1 \end{bmatrix}$	40	ZF/ICD	5

#### E. Receiver and Detector

A Zero Forcing (ZF) / Inverse Channel Detector (ICD) [6] with minimal Euclidian distance decision was employed, because of its linearity and the simplicity of the implementation.

The worse the transmission matrices are conditioned ( $\kappa \gg 1$ ), the higher is the intrinsic noise enhancement of the receiving algorithm [8]. This enhancement has to be overcome by a higher downlink power  $P$  to achieve a certain data throughput  $y$ .

#### F. Receiver and Detector

The downlink power used for the simulation ranges from -130dBm to -50dBm. It is always related to a subcarrier bandwidth of 15kHz.

The noise signals are added after the antenna matrices. Noise energies are always related to the channel bandwidth (15kHz). The noise figure of the UE was assumed to be 5.2dB, as this is a characteristic number of a user equipment employed in the CTIA (The Wireless Association) round robin measurement campaign.

#### G. Number of Realizations

A realization is the transfer of transmission data block ( $2^8$  bits). In general, 5000 of those were simulated. The higher this number, the smoother are the downlink power vs. throughput curves  $P(y)$ .

## IV. INVESTIGATION RESULTS

In this section the results of the investigations are

presented. They range from simple system tests to complete transmission simulations:

- System test with identity antenna matrix (Fig. 3)
- Simulation with complete channel matrices and different antenna condition number  $\kappa$  (Fig. 4 and Fig. 5).

The parameters of the transmission systems including channel and antenna matrix, condition number of the antenna matrix  $\kappa$  and the corresponding result figures are presented in Table I.

A representative selection of antenna condition numbers has been chosen (0dB, 10dB and 40dB). It shows the rise of the deviation with rising condition numbers very well (Fig. 3, Fig. 4 and Fig. 5). The curves show downlink power  $P$  as a function of the relative throughput (RTP)  $y$ . An RTP of 1 means all data is transferred correctly, 0 means not a single subframe transmission can be achieved.

The magenta curves (marked with \*) show the decomposition result  $P_{dc}(y)$  (Fig. 3, Fig. 4 and Fig. 5). Naming conventions are taken from section II. The 'Baseline' results  $P_{bl}(y)$  are equal in all three simulations and represent the best reachable sensitivity with a steeply rising RTP  $y$ .

The 'Channel' results  $P_{ch}(y)$  show a less steep increase due to the Rayleigh distribution of the channel matrix elements.  $P_{ant}(y)$  is a parallel right shifted version of  $P_{bl}(y)$ , due to degradation of the receiver by intrinsic noise enhancement of the receiving algorithm.

$P_{oa}(y)$  is the specified value,  $P_{dc}(y)$  is the actual value. The deviation between both is calculated by

$$deviation_{log} = P_{dc,log}(y) - P_{oa,log}(y)$$

The results of simulation are shown in Fig. 3. It employs a perfect antenna matrix with  $\kappa = 0$ dB and a channel matrix as described in III-C. The 'Antenna' simulations are congruent with the 'Baseline'. The 'Channel' result has a less steep slope due to the complex normal distribution of the channel elements. It is the same in all three simulations (Fig. 3, Fig. 4 and Fig. 5). The 'Overall' and the 'Decomposition Method' result curves are completely congruent.

Fig. 4 exhibits the results at  $\kappa = 10$ dB. The 'Antenna' and the 'Overall' curve show less sensitivity due to the starting noise enhancement of the receiver.

Fig. 5 points out the behavior for  $\kappa = 40$ dB, which is representative for an antenna system with strong coupling between the antennas. Even stronger noise enhancement is taking place. It has to be overcome by higher downlink power. The deviation of 'Overall' and 'DC Method' result has become bigger (-0.54dB). The 'Overall' and the 'Decomposition Method' results start to deviate, although still with low deviation (-0.2dB at an RTP of 0.7).

As stated the downlink power has to increase with ascending antenna condition numbers. The simulations also show that the deviation between 'Decomposition Method' results  $P_{dc}(y)$  and 'Overall' results  $P_{oa}(y)$  becomes bigger with rising antenna condition numbers  $\kappa$ .

Table II shows these nominal offsets with the corresponding condition numbers. The maximum deviation is -0.54dB, so to say the method is valid for the ICD/ZF receiver for the given circumstances within this error range. From RF measurement practice it can be stated, one can live

with that magnitude of error, as the measurement setup uncertainties will also be within this margin.

TABLE II: DEVIATION BETWEEN 'DC-METHOD' AND 'OVERALL' RESULT

ant. cond. nr. /dB	deviation (DC-OA) / dB	Fig.
0	0	3
10	-0.2	4
40	-0.54	5

## V. CONSIDERATIONS OF DEVIATION USING REFERENCE ANTENNAS

The last section describes the behavior of the decomposition method in practical usage. It summarizes the impact of using the method with a typical MIMO antenna system pattern. A good practical example is the set of LTE reference antennas defined by CTIA for band 13 (751MHz) [9]. These reference antennas allow to compare the performance of different UEs without their own antennas. Originally it was used in CTIA round robin tests for evaluating different test methodologies. It consists of three overall performance types:

- "good"
- "nominal"
- "bad"

Antenna characteristics as S-parameters, impedance, far field pattern, gain imbalance, magnitude of complex correlation coefficient, can be seen in [9]. An OTA performance measurement of a UE consists of many different constellations. The applied constellation set contains 128 positions and can be seen in [10]. To avoid oversampling at the poles of the spherical coordinate system, the angle distribution is based on the golden angle of  $137.508^\circ$  [10].

The distribution of the condition number  $\kappa$  over the constellations is indicated in Fig. 6. The x-axis exhibits the log. UE antenna condition number, the y-axis shows the constellation counts within the range of the shown bins of  $\kappa$ . The logarithmic mean value of  $\kappa$  is rising going from antenna type 'good' over 'nominal' to 'bad'. This reflects the design intention of the reference antennas.  $\kappa$  is dependent on the antenna constellation and strongly influences the receiver performance. It is interesting to see how a histogram of the condition number of all constellations (Fig. 7). As expected the logarithmic mean value of  $\kappa$  is rising going from 'good' to 'bad' reference antenna.

The deviation between the 'Decomposition Method' result and the 'Overall' result has been calculated for all RX antenna matrices defined by the antenna patterns and constellations (as calculated in section IV). For the ZF/ICD receiving algorithm it can be seen in Fig. 7. The logarithmic mean values can be found in Table III. Results have been calculated for RTP = 0.7. This equals 70% relative throughput.

The investigations show that in practice the mean deviation is even lower than the maximum values (e.g. -0.35dB for the 'bad' antenna compared to -0.54dB with 40dB ant. cond. number). This lowered mean deviation is caused by the varying condition numbers of the used antenna constellations. Their mean value does not reach the maximum values. For practical purposes this implies a reduced error range in the case of the LTE reference antennas usage.

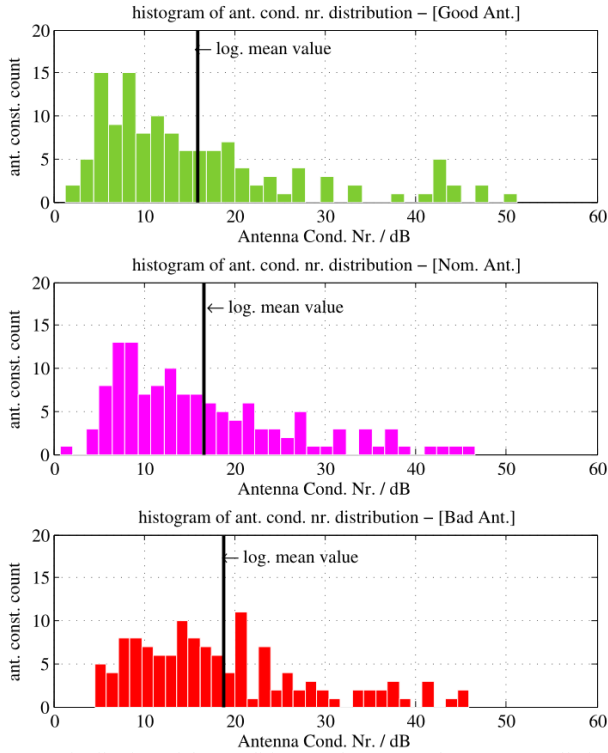


Fig. 6. Distribution of the condition number  $\kappa$  over the ant. Constellations and antenna types — ZF receiver.

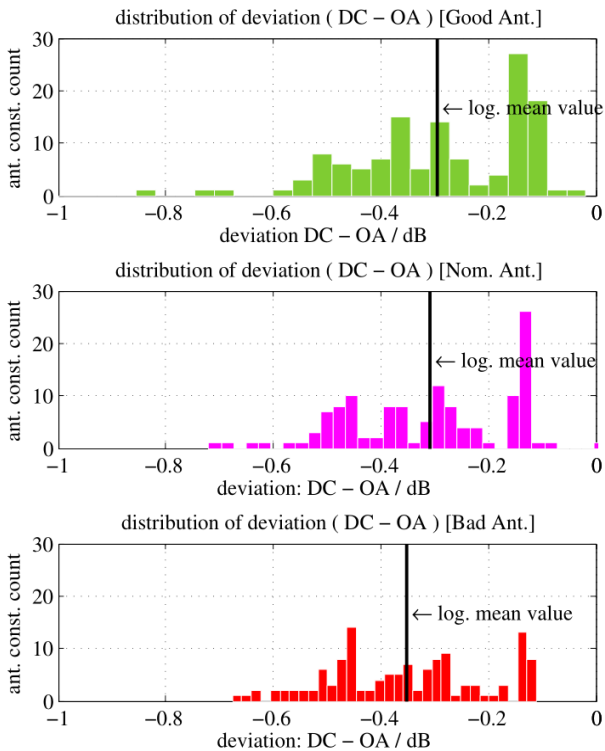


Fig. 7. Distribution of the deviation (DC - OA) over the antenna types and constellations — ZF receiver.

TABLE III: MEAN DEVIATION FOR DIFFERENT REFERENCE ANTENNA TYPES

Reference antenna type	mean cond. nr. /dB	mean deviation (OA - DC) /dB
Good	15.9	-0.29
Nominal	16.6	-0.31
Bad	18.7	-0.35

## VI. CONCLUSION

A numerical validation of the decomposition method

within the given limitations has been shown in this paper. For this purpose a  $2 \times 2$  MIMO transmission system with an ICD/ZF receiver has been employed. The used modulation scheme was QPSK, the channels were flat frequency fading. The simulation results show a good agreement between the decomposition method result and the 'Overall' result. The deviation starts from 0dB and rises with increasing condition number of the antenna. These limiting factors can be shown well with the basic setup.

The mean deviation does not reach the maximum values when a practical antenna system like the LTE reference antennas is used. The reason for this is the distribution of the antenna condition numbers, that are below also the maximum value.

## VII. FUTURE WORK

One of the next steps is to introduce more complex channel models like tapped delay models. Also the modulation and coding scheme (MCS) should become more sophisticated and contain all necessary elements from more complex protocols like LTE.

## ACKNOWLEDGEMENT

The authors would like to thank Hasan Noor Khan and Philipp Freidl, TU Graz, for fruitful technical discussions and literature recommendations.

## REFERENCES

- [1] C. Gagern, A. Tankielun, Y. Feng, and T. Hertel, "Decomposition test results from the second CTIA round robin test," in *Proc. COST IC1004*, Ilmenau, Germany, 2013.
- [2] 3GPP, "Verification of radiated multi-antenna reception performance of user equipment (UE)," January 2014.
- [3] A. Tankielun, "Two-channel method for OTA performance measurements of MIMO-enabled devices," Rohde and Schwarz White Paper, 2011.
- [4] Rohde and Schwarz, "Two-channel method for evaluation of MIMO OTA performance of wireless devices," presented at 3GPP Meeting, Jacksonville, November 15, 2010.
- [5] C. W. Sirles, J. C. Mantovi, A. R. Howland, and B. J. Hart, "Anechoic chamber performance characterization using spherical near-field imaging techniques," in *Proc. 3rd European Conference on Antennas and Propagation*, March 23-27, 2009, pp. 1734-1738.
- [6] J. Proakis and M. Salehi, *Digital Communications*, 5th ed. McGraw-Hill, 2008.
- [7] B. Auinger, A. Tankielun, M. Gadringer, C. Gagern, and W. Boesch, "Introduction of a simulation approach for the two-channel method using system VUE," in *Proc. COST IC1004*, 2013.
- [8] J. Barry, E. Lee, and D. Messerschmitt, *Digital Communication*, 3rd ed. 2004 Springer Science & Business Media, Inc.
- [9] I. Szini, "Reference antennas proposal for MIMO OTA," in *Proc. COST IC1004 2nd MCM*, Lisbon, Portugal, Oct. 2011.
- [10] A. Tankielun and C. V. Gagern, "On spatial characteristics of the decomposition method in MIMO OTA testing," in *Proc. 2014 8th European Conference on Antennas and Propagation*, the Hague, Netherlands, 2014, pp. 3674-3678.

**Bernhard Auinger** received the master degree in electrical engineering (Dipl. Ing.) from Graz University of Technology in 2004. From 2005 to 2011, he initiated and ramped up the electromagnetic compatibility group for automotive ICs at Philips Semiconductors and NXP Semiconductors. Since 2011 he has been a university assistant at the Institute of Microwave and Photonic Engineering at the Graz University of Technology.

During his studies he was engaged in the comet mission ROMAP/ROSETTA of the European Space Agency (ESA). His current research activities are theoretical investigations for wireless communications and on test procedures for MIMO enabled user equipment.

**Michael Gadringer** received the Dipl.-Ing. and the Dr.techn. degrees from the Vienna University of Technology in 2002 and 2012, respectively. Since 2010 he is a university assistant at the Institute of Microwave and Photonic Engineering at the Graz University of Technology. During his studies he was involved in the design of analog and digital linearization systems for power amplifiers and with the behavioral modeling of microwave circuits. His current research activities focus on the design and linearization of broadband microwave and mm-wave communication systems as well as on measurement techniques and de-embedding. He has co-edited the book *RF Power Amplifier Behavioral Modeling* published by Cambridge University Press.

**Adam Tankielun** received his master and Dr.-Ing. degrees in electrical engineering from the Technical University of Gdańsk in 2002 and the Leibniz University of Hannover in 2007, respectively. From 2003 to 2008, he developed electromagnetic near-field scanning techniques for the Fraunhofer Institute for Reliability and Microintegration in Paderborn. Since 2008 he has been with Rohde & Schwarz GmbH & Co. KG in Munich developing over-the-air test systems for wireless devices.

**Christoph von Gagern** joined Rohde & Schwarz, Munich, Germany, in 1985. Since 1991 he was active in the area of EMC projects, and was the head of R&D EMC Systems and Projects since 1999. Areas of his work cover EMC test systems with the focus on immunity testing, over-the-air antenna performance measurement systems, and EMF environmental testing systems. He is a member of the CIS/I subcommittee on information technology equipment, multimedia equipment and receivers with its working groups, and also of standardization bodies for OTA testing like 3GPP RAN WG4 or CTIA.

**Wolfgang Bösch** has joined the Graz University of Technology in Austria to establish a new Institute for Microwave and Photonic Engineering, in March 2010. Prior he has been the CTO of the Advanced Digital Institute in the UK, a non-profit organization to promote research activities. He had also been the director of Business and Technology Integration of RFMD UK. For almost 10 years he has been with Filtronic PLC as the CTO of Filtronic integrated products and the director of the Global Technology Group. Prior to joining Filtronic, he held positions in the European Space Agency (ESA) working on amplifier linearization techniques, MPR-Teltech in Canada working on MMIC technology projects and the Corporate R&D group of M/A-COM in Boston where he worked on advanced topologies for high efficiency power amplifiers. For four years he was with DaimlerChrysler Aerospace in Germany, working on T/R Modules for airborne radar.

Dr. Bösch received his engineering degree from the Technical University of Vienna and Graz in Austria. He finalized his MBA with distinction at Bradford University School of Management in 2004. He is a fellow of the IEEE and a fellow of the IET. He published more than 50 papers and holds 4 patents. He was a non-executive director of Diamond Microwave Devices (DMD) and is currently a non-executive director of the Advanced Digital Institute (ADI) and VIPER-RF company.